NANO LETTERS

2008
Vol. 8, No. 8
2393-2398

Nanoelectromechanical Switch Operating by Tunneling of an Entire C_{60} Molecule

Andrey V. Danilov,[†] Per Hedegård,[‡] Dmitrii S. Golubev,[§] Thomas Bjørnholm,[*,‡] and Sergey E. Kubatkin[†]

Department of Microtechnology and Nanoscience, Chalmers University of Technology, Fysikgränd 3, S-41296 Göteborg, Sweden, Nano-Science Center (Niels Bohr Institute & Department of Chemistry), University of Copenhagen, Universitetsparken 5, DK-2100 Copenhagen, Denmark, and Forschungszentrum Karlsruhe, Institut für Nanotechnologie, 76021 Karlsruhe, Germany

Received May 5, 2008; Revised Manuscript Received June 16, 2008

ABSTRACT

We present a solid state single molecule electronic device where switching between two states with different conductance happens predominantly by tunneling of an entire C_{60} molecule. This conclusion is based on a novel statistical analysis of $\sim 10^5$ switching events. The analysis yields (i) the relative contribution of tunneling, current induced heating and thermal fluctuations to the switching mechanism, (ii) the voltage dependent energy barrier ($\sim$100−200 meV) separating the two states of the switch and (iii) the switching attempt frequency, ω_0, corresponding to a 2.8 meV mode, which is most likely rotational.

Fundamental studies of electronic transport between electrodes separated by a single molecule are crucial for the future development of molecular electronics and it has been the subject of a number of recent studies.[1–3] One particularly fascinating aspect of such devices is the possibility of exploiting molecular degrees of freedom to realize basic functionalities like switching.[4–22] By default, molecular degrees of freedom (electronic as well as vibronic) are determined by quantum mechanics. In the present paper we focus on the intriguing possibility that quantum motion of the entire molecule may also play a role in the switching process.

The first example of such a switching device was the Eigler switch operated by tunneling of a Xe atom between a metal surface and an STM tip.[23] Because tunneling is a quantum process the probabilistic nature of quantum mechanics presents new challenges to operate such devices. For example, the switching event *per se* will be subject to quantum fluctuations resulting in dispersion of the switching voltages.

In this paper we present a new switch consisting of a single C_{60} molecule located in the nano gap between two silver electrodes. At low temperatures the device switches between two states with different conductance. By analyzing the distribution of switching voltages, we are able to extract the key device parameters such as the barrier separating the two states of the switch, the attempt frequency etc.

C_{60} as an experimental test system has the advantage of being well characterized in previous studies. The electronic as well as vibronic structure of the C_{60} molecule is well-known from experiments[24–26] and first principle calculations.[27,28] Electron transport through C_{60} has been extensively studied in STM experiments. Already in the 1990s the transconductance of a single C_{60} on Cu was measured[29] and more recently a similar study of C_{60} on silver was presented.[30,31]

In our experiments the C_{60} molecules were placed into a nanogap prepared in an UHV environment by quench condensation of metallic electrodes onto a substrate held at 4 K, as described in detail in previous publications.[7,32–34] An approximately 2 nm wide gap between silver electrodes is evaporated onto an aluminum oxide covered aluminum gate electrode through a mask elevated above the surface. The resulting tunneling gap is carefully characterized.[33,35] Next, in the same vacuum cycle, the C_{60} molecules are sublimated from a second evaporator typically in $\sim$1% of monolayer coverage. At 4 K, the molecules get stuck at the sites where they initially contact the aluminum oxide surface. After completion of the molecule deposition, the $I-V$ characteristic of the gap remains unchanged, indicating that no molecules

* To whom correspondence should be addressed. E-mail: tb@nano.ku.dk.
† Chalmers University of Technology.
‡ University of Copenhagen.
§ Institut für Nanotechnologie.

10.1021/nl801273a CCC: $40.75
Published on Web 07/22/2008

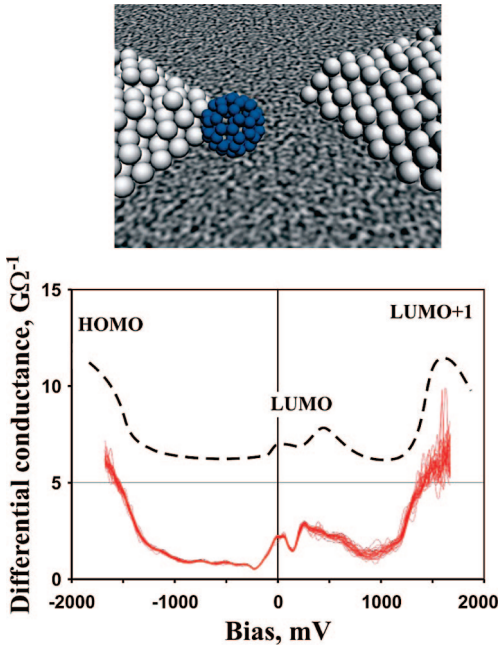

Figure 1. Top: sketch of a C_{60} molecule between two silver electrodes. Due to the absence of Coulomb blockade behavior the molecule is most likely attached to one of the electrodes as shown. Bottom: differential conductance for C_{60} trapped in a silver gap. Solid red curves: 32 representative curves for high-conducting state.[36] Dashed line: sketch of the STM data reported in refs 30 and 31 (scaled 10 times and shifted vertically for clarity), where individual fullerenes on a silver substrate were directly imaged in UHV. Note similar position of the maxima corresponding to different molecular orbitals (HOMO, LUMO and LUMO+1).

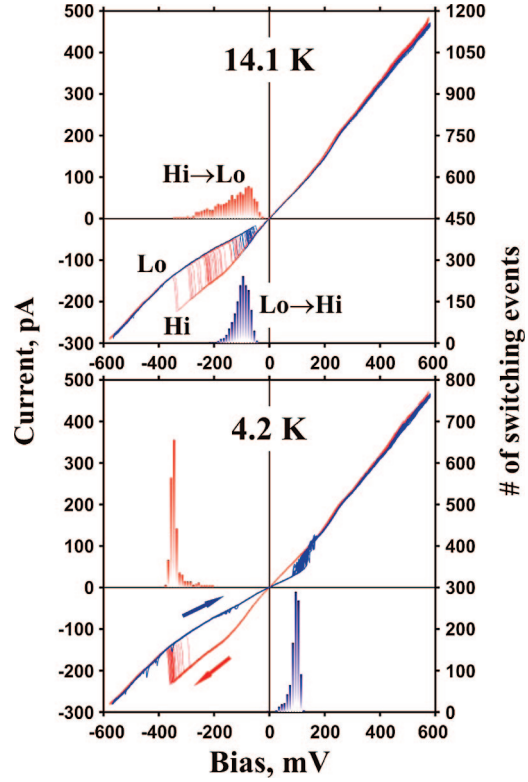

Figure 2. Current−voltage characteristics at two different temperatures. The bias voltage was ramped at 150 mV/s. For every temperature the 32 representative voltage ramps are shown. For the blue curves voltage was swept from negative to positive bias, and for the red curves the bias was swept in the opposite direction. Inserted are the histograms of the switching events.

have evaporated directly into the gap. In the last step, one molecule is trapped in the gap by applying a bias across the gap while annealing at about 60 K. The combination of electrostatic attraction to the gap and thermally induced mobility of the molecules allows one of the widely spaced molecules deposited on the aluminum oxide surface to diffuse into the gap. Once the first molecule is trapped, a dramatic change in the current flowing across the gap is observed. At this point, the device is cooled back to 4 K, and detailed measurements are performed.

We have fabricated five C_{60} devices with gold electrodes[33] and two with silver electrodes; they all showed qualitatively similar behavior. In this paper we focus on one sample with silver nanogap, which we have chosen for a detailed study of switching kinetics.

Our fabrication method ensures a clean contact between the molecule and metallic electrode due to the unbroken vacuum.[32–34] As a result, our C_{60} devices with silver electrodes display *quantitatively* the same spectroscopic features reported in UHV STM studies of C_{60} on silver.[30,31] The data in the bottom panel of Figure 1 is a fingerprint of C_{60} on silver and provide direct experimental evidence that we can trap a single fullerene in the UHV-grade nanogap.

The *IV* characteristics, including the absence of a gate effect, indicate that the C_{60} molecule is positioned very asymmetrically in the metallic nanogap interacting strongly with the electrode that it is in direct contact to, and weakly with the other due to the presence of $a \approx 1$ nm tunneling gap. The whole geometry of the single molecule switch is hence very similar to the STM setup. However, far better temperature- and time-stability of our nanogaps allowed long-term measurements, unconceivable in the STM geometry.

While the high bias scan shown in Figure 1 allows direct comparisons to electronic features observed in STM experiments, Figure 2 displays a typical sample of the raw data underlying the following analysis. Scans in this more narrow bias window yielded very reproducible results allowing the temperature dependence of switching histograms in both scanning directions (Figure 2 red/blue) to be sampled for an extended period of time (6 weeks).

In our analysis of this data we extend the procedure previously described in ref 7. We consider a bistable system, where the two states (we shall call them "Hi" and "Lo", according to the value of the current through the molecular junction) are separated by some potential barrier. For the negative to positive bias sweeps the switch is initially in the "Lo" state (see Figure 2) and will eventually switch to the "Hi" state. The probability density that a switching event will occur at a given time t is given by $P_S(t) = \Gamma_{LH}(V(t))\, Q(t)$. Here $\Gamma_{LH}(V)$ is the bias (and temperature) dependent rate for going from the state "Lo" to the state "Hi", and $Q(t)$ is the probability a switching event has *not* occurred prior to time t. $Q(t)$ satisfy the simple rate equation

$$\frac{\mathrm{d}}{\mathrm{d}t}Q(t) = -\Gamma_{\mathrm{LH}}(V(t))\, Q(t) \tag{1}$$

This is easily solved and we get

$$P_{\mathrm{S}}(t) = \Gamma_{\mathrm{LH}}(V(t)) \exp[-\int_{t_0}^{t} \Gamma_{\mathrm{LH}}(V(t'))\, \mathrm{d}t'] \tag{2}$$

Because the *IV* characteristics are recorded by scanning the bias voltage at a certain sweep rate u so that $V(t) = V_0 + u(t - t_0)$, the switching probability can be given in terms of V:

$$\widetilde{P}_{\mathrm{S}}(V) = \frac{\Gamma_{\mathrm{LH}}(V)}{u} \exp\left[-\int_{V_0}^{V} \frac{\Gamma_{\mathrm{LH}}(V')}{u}\, \mathrm{d}V'\right] \tag{3}$$

Equation (3) can be solved for $\Gamma_{\mathrm{LH}}(V)$:[37]

$$\Gamma_{\mathrm{LH}}(V) = u \frac{\widetilde{P}_{\mathrm{S}}(V)}{1 - \int_{V_0}^{V} \widetilde{P}_{\mathrm{S}}(V')\, \mathrm{d}V'} \tag{4}$$

In other words, from the measured distribution $\tilde{P}_{\mathrm{S}}(V)$ of the switching events one can find the underlying switching rate $\Gamma_{\mathrm{LH}}(V)$ in a straightforward manner.

Following this procedure Figure 3 presents the distribution of "Lo" → "Hi" switching events, measured at different temperatures from 4.2 to 22.9 K together with the corresponding switching rates. At higher temperatures the switching happens at lower voltages, i.e., earlier in time. This means that temperature promotes switching. Also, at any given temperature the switching rate increases with the bias voltage. As the simplest model that accounts for both experimental findings, one can consider the temperature-induced switching over a voltage dependent barrier with a switching rate $\Gamma_{\mathrm{LH}}(V) = \omega_0 \exp(-\Delta(V)/k_{\mathrm{B}}T)$. By plotting $-k_{\mathrm{B}}T \ln(\Gamma_{\mathrm{LH}}(V))$, we

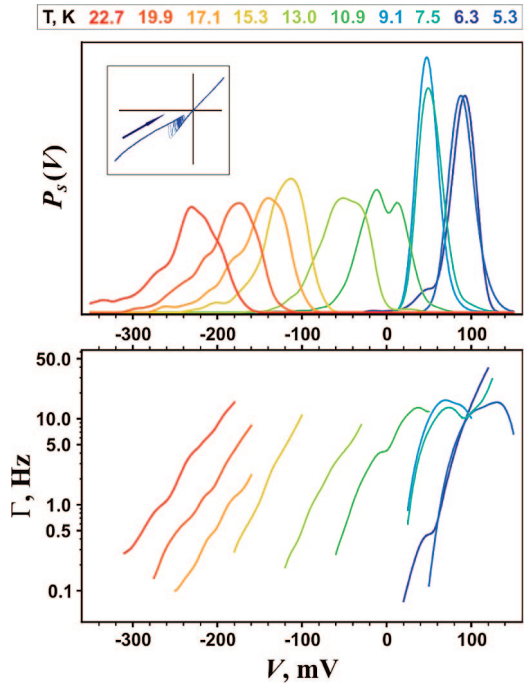

Figure 3. Top: observed probability that the system will switch from state "Lo" to state "Hi" at a certain voltage, when the voltage is swept from negative to positive voltages. Each observed switching voltage is represented as a Gaussian with width 5 meV, and all these Gaussians are added. Bottom: escape rates generated using (4).

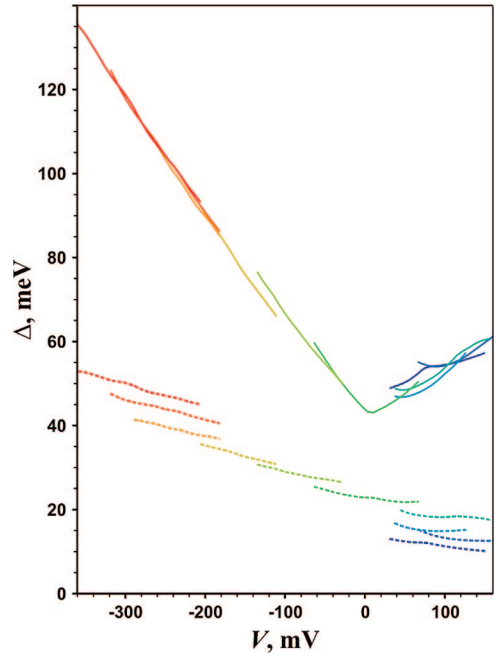

Figure 4. Dotted lines: barrier height, $\Delta(V)$, as a function of voltage, derived from the switching data (same color coding as in Figure 3) in a simple Arrhenius model. The value of the attempt frequency is such that $\hbar\omega_0 = 3$ meV. Solid lines: barrier $\Delta(V)$ determined from the experimental escape rates using a refined model that includes quantum tunneling and current induced heating through one additional parameter $\alpha = 7.1 \times 10^{-3}$; $\hbar\omega_0 = 2.8$ meV (*cf.* text).

can try to reconstruct the barrier height $\Delta(V)$ as a function of voltage. The result is shown in Figure 4 with dotted lines.

The model implies that the barrier height should be independent of temperature. The result contradicts this assumption because there is no common $\Delta(V)$ barrier for all temperatures. We thus need a more refined model, which we shall turn to now.

We note first that the typical energies of mass-center (vibrational or rotational) oscillations of C_{60} trapped in a metallic nanogap are about a few millielectronvolts,[38] which is not negligible compared to the experimental temperatures ($\approx$0.2−1 meV). In fact, below ~10 K, the characteristic C_{60} energy is essentially the energy of ground-state fluctuations, and not $k_{\mathrm{B}}T$, as for the Arrhenius model. This may be the reason why the Arrhenius model fails to explain the data and in the refined model we shall consider C_{60} as a quantum object.

Without specifying the nature of "Hi" and "Lo" states, we assume that there is some coordinate, x, associated with switching, which we will refer to as a "reaction coordinate". This coordinate is not necessarily a Cartesian coordinate; it may well be an angle. In the following we shall use a notation as if it is a Cartesian coordinate. If, however, it is an angle, quantities like mass should be replaced by moments of inertia. The energy landscape along the reaction coordinate is sketched in Figure 5.

For simplicity we shall assume that the potential is harmonic out to a coordinate, R_{c}, and that the system will

escape if it makes it beyond this point. The escape rate is therefore proportional to the probability to find the C_{60} at $x = R_c$.

At zero temperature this probability is defined by the ground-state dispersion $\langle R_0^2 \rangle$:

$$\Gamma_{LH}(V) \propto \exp\left[-\frac{R_c^2}{2\langle R_0^2\rangle}\right] = \exp\left[-\frac{\Delta}{E_0}\right] \tag{5}$$

where Δ is the barrier height, E_0 is the ground-state energy, and we used the fact that for harmonic oscillator

$$\begin{aligned} \Delta &= \frac{1}{2} m\omega_0^2 R_c^2 \\ E_0 &= \frac{1}{2} m\omega_0^2 \langle R_0^2 \rangle \end{aligned} \tag{6}$$

At finite temperature the ground-state energy E_0 in (5) should be replaced with the time-average energy of the oscillator coupled to a heat bath:[39–41]

$$\langle E(T) \rangle = \frac{\hbar\omega_0}{2} \coth \frac{\hbar\omega_0}{2k_B T} \tag{7}$$

Note that at high temperatures ($k_B T \gg \hbar\omega_0$), $\langle E(T) \rangle \rightarrow k_B T$ and the switching rate reduces to the Arrhenius law, whereas in the opposite case of $T \rightarrow 0$ the oscillator energy approaches $^1/_2\hbar\omega_0$ and the quantum result is recovered.

The last ingredient we will add to the model is the heating associated with a current running from one electrode to the other through the molecule. This is in part motivated by the fact that for $T = 11.6$ K the switching events are taking place around voltage $V = 0$ (see Figure 3). The observed probability has a pronounced dip at zero bias, i.e., when little or no current is moving through the system. This suggests that the current actually is helping the system getting over the barrier the more the voltage and the associated current is different from zero.

When an electron is added to C_{60}, the equilibrium position of the reaction coordinate is shifted by some amount, and the coordinate experiences a force. When the extra electron leaves the molecule, the original equilibrium position is restored, but an amount of energy is transferred to the C_{60} in the process. A model containing similar physics was used in the analysis of the Eigler switch,[40,41] where it was shown that in the presence of a transport current the time-average oscillator energy reads:

$$\langle E(T,V) \rangle = \frac{\hbar\omega_0}{2} \coth\left(\frac{\hbar\omega_0}{2k_B T}\right) + \alpha(|eV| - \hbar\omega_0)\theta(|eV| - \hbar\omega_0) \tag{8}$$

where $\alpha = (G/e^2)(\bar{E}/\eta)$; G is the sample conductance, $\bar{E}$, is the average energy supplied by one tunneling electron, and η is the relaxation rate of the mechanical oscillations. The current-induced correction to the average energy is therefore the energy supplied by passing electrons during the relaxation time of vibrations associated with the reaction coordinate; the θ-function in (8) accounts for the fact that electrons can not excite the reaction coordinate if the bias-supplied energy $eV < \hbar\omega_0$. One can show (see the Supporting Information for the detailed calculations) that in the presence of transport current the escape rate is given by (5) with an average energy $\langle E \rangle$ in the generalized form (8).

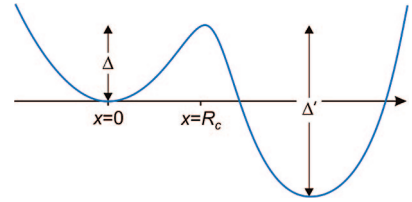

Figure 5. Simple model for the energy landscape along the reaction coordinate. The metastable well corresponds to the state "Lo".

Assuming an attempt rate $\sim\omega_0/2\pi$ we arrive at the model with just two fitting parameters: ω_0 and α. For any given choice of (ω_0, α) we can reconstruct the barrier height $\Delta(V) = -\langle E(T,V) \rangle \ln (2\pi\Gamma_{LH}(T,V)/\omega_0)$ from the switching rate $\Gamma_{LH}(T,V)$ measured at temperature T. As shown in Figure 4, with a proper choice of fitting parameters ($\hbar\omega_0 = 2.8$ meV, $\alpha = 7.1 \times 10^{-3}$), all the $\Delta(V)$ plots collapse into a single curve. This is the key result of our data analysis. In the following we treat it as experimentally determined temperature-independent barrier $\Delta(V)$.

Because our model (eq 8) includes thermal, quantum and current induced effects we are able to estimate the relative contribution of these effects to the over all "Lo"−"Hi" switching process. This exercise shows that at low temperatures tunneling is indeed the dominant switching mechanism. At 4 K and 100 mV bias, for example, the different contributions to the total oscillator energy are according to eq (8): 1.4 meV from the quantum mechanical ground-state oscillations, ~0.001 meV from the thermal fluctuations and 0.7 meV from the current-induced heating.

Knowing the oscillator frequency $\omega_0 \approx 4.2$ THz, we can estimate the mass of the tunneling object. As it was discussed, at low temperatures the dominant switching mechanism is tunneling, and one can use a simplified formula (5) to estimate the dispersion of the ground state $\langle R^2 \rangle = R_c^2/\ln(\omega_0/2\pi\Gamma)$. As the switching actually happens when Γ is in the range ~1−10 Hz (Figure 3), we can estimate the logarithm in the former formula as ~25, and the tunneling mass $m = \hbar/\omega_0\langle R^2 \rangle \approx 25\hbar/\omega_0 R_c^2$. The maximum possible value for $R_c \sim 0.3$ Å can be estimated from the fact that the sample conductance in Figure 2 only changes by a factor of 2, and we arrive at $m \geq 400 m_p$ (m_p is the proton mass). This rules out all switching mechanisms involving the displacement of silver atoms in the electrodes and corroborates a tunneling process involving a mass in the C_{60} range.

So far, we have made no detailed assumptions about the nature of the reaction coordinate. The oscillator energy of $\hbar\omega_0 = 2.8$ meV is too small to be assigned to any internal vibration mode of the C_{60} molecule,[42] so we shall associate the reaction coordinate with rotation or displacement of the entire C_{60} molecule. The latter we can exclude as well, because the energy required for the lateral C_{60} displacement is ~800 meV,[43] which is well above the observed barrier height of 40−140 meV. On the other hand, the barrier for C_{60} rotations, which was calculated to be 90 meV for C_{60} on Au(110)[44] and experimentally found to be 58 meV in a C_{60} film[45] is in the right range.

The minimum in $\Delta(V)$ at $V = 0$ in Figure 4 could be a simple electrostatic effect because the device is in essence a

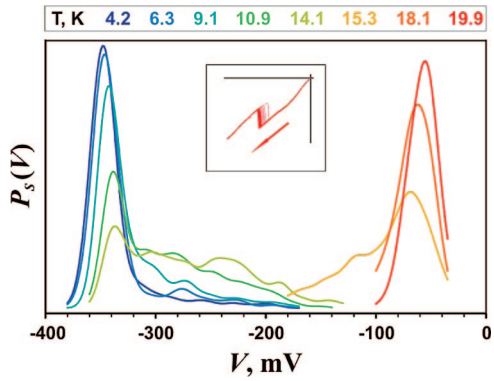

Figure 6. Probability of switching when the voltage is swept from positive to negative voltages.

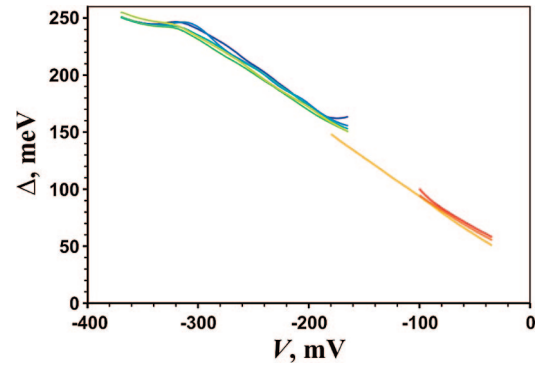

Figure 7. Barrier height, Δ', extracted from the data assuming the switching rate is of the form $\Gamma \propto e^{-\Delta'/k_B T_{eff}}$ with an effective temperature determined by current generated heating (through coupling to the vibration mode with $\hbar\Omega = 35$ meV) and quantum effects. Temperatures as in Figure 6. The parameter $\hbar\omega'_0$ is 2.5 meV, $\alpha' = 0.02$.

capacitor obeying the electrostatic relation $U = {}^1/_2 C(x)V^2$, where the capacitance $C(x)$ depends on the reaction coordinate, x, of C_{60}. Following this analysis, the change in capacitance, $\Delta C(x)$, resulting from switching is reflected in the scales in Figure 4, and a rough estimate yields $\Delta C(x) \approx 1 \times 10^{-19}$ F, which is a fraction (≈20%) of the capacitance of a C_{60} molecule on an aluminum oxide surface. However, this simple analysis does not account for the linear asymptotes for both positive and negative biases on Figure 4. This may be related to the simplified model we have used for the effects of transport current.

Finally, we shall discuss switching in the opposite direction. The switching histograms for "Hi" → "Lo" transition are shown in Figure 6. As in the "Lo" → "Hi" case, we find that a simple Arrhenius model does not give a reasonable representation of the data. A refined model (5–8), which includes quantum effects and heating due to current, gives a satisfactory fit if we assume that the current induced heating starts from the threshold bias of 35 meV. In fact, from the raw histograms in Figure 6 one can clearly see that the backward switching is mediated by excitation of the 35 mV mode: at the three highest temperatures the switching histograms have a clear onset at approximately 35 mV.

For "Lo" → "Hi" switching we assumed that the 2.8 meV vibration mode associated with the reaction coordinate is coupled directly to the tunneling electrons. This need not be the most general scenario. Some vibrational modes with higher energies may in fact be stronger coupled to the moving electrons. This energy may then, through the intermode coupling, "triggle down" to the reaction coordinate and ultimately help the system to pass over the energy barrier. It is known that the charged C_{60} molecule is Jahn−Teller distorted. The Jahn−Teller active modes are the ones with the highest electron−phonon coupling, the energy of the lowest Jahn−Teller active mode $H_g(1)$ for C_{60} in vacuum is around 34 meV,[46,47] it seems to be natural to associate the mediating coordinate with this breathing mode.

A detailed model, which includes the reaction coordinate, oscillating in a quadratic minimum like in Figure 5 with a frequency ω_0', which gains energy through the coupling to a "helper" coordinate, oscillating with frequency Ω, and dissipates energy into the reservoir, is considered in the supporting material. It is shown there that the current-induced heating for this model has a threshold at $|eV| = \hbar\Omega$ and is approximately linear above the threshold. The total energy of the oscillator associated with reaction coordinate is then

$$\langle E(V,T)\rangle = \frac{\hbar\omega_0'}{2}\coth\left(\frac{\hbar\omega_0'}{2k_B T}\right) + \alpha'(|eV| - \hbar\Omega)\theta(|eV| - \hbar\Omega) \tag{9}$$

where the renormalized coupling constant α' implicitly includes the inter mode coupling.

The reconstructed barrier height for backward switching is shown in Figure 7.

The 35 mV mode is active in the ground state and inactive in the metastable state. It is this asymmetry that makes the device bistable. Apparently the coupling between the breathing mode and the reaction coordinate is rather different for two states.

The analysis so far does not reveal the precise nature of the two switch states, and the reaction coordinate connecting the two. We may speculate that they are associated with configurations, where either a pentagon or a hexagon of carbon atoms are facing and contacting the metal electrode. In this case the reaction coordinate is indeed an angle, and the oscillator is some rotation mode, with a frequency as small as 2.8 meV. This scenario also offers a natural explanation for the different couplings to the Jahn−Teller distortion. When the hexagon faces the metal the Jahn−Teller distortion goes in the direction normal to the surface and coupling to the rolling vibrations should be suppressed by symmetry. We therefore conclude that in such a scenario, the "Hi" state corresponds to a pentagon facing the metal electrode.

In summary, statistics of $\sim 10^5$ of switching events of a single bistable fullerene (C_{60}) molecule trapped between silver electrodes has been collected for a device which was stable for over 6 weeks. The data were collected in the millisecond time domain at temperatures between 2 and 20 K and currents ranging between 0 and 500 pA for both directions of switching. The entire data set is analyzed in a model invoking simple Arrhenius type activation as a starting point for calculating the switching rate, $\Gamma = \omega_0 \exp(-\Delta/$

$\langle E \rangle$). It is shown that current induced heating as well as quantum tunneling needs to be included to encompass all the data in the same model. Data analysis reveals a bimodal energy landscape with a voltage dependent barrier ($\approx$100−200 meV) separating the two states of the switch. It is shown that quantum tunneling is the dominant mechanism for switching in one direction, and switching in the opposite direction is additionally assisted by a current induced excitation of the 33.7 meV breathing mode of C_{60}. In both directions the attempt frequency, ω_0, corresponds to 2.8 meV (rotational) mode. This scenario is consistent with a simple mechanical switching mechanism where C_{60} rolls from one orientation to the other and it provides a benchmark for the relevance of quantum mechanics in relation to nanoelectromechanical (NEMS) switching.

Acknowledgment. We are grateful to E. Campbell and M. Heden for mass-spectrum test of C_{60} evaporator, and to K. Flensberg for inspirational discussions. The work was supported in part by European Community's Seventh Framework Programme (FP7/2007-2013) under grant the agreement "SINGLE" no 213609 and through project FP6-003673 CANEL of the IST Priority. (The views expressed in this publication do not necessarily reflect the official European Commission's view on the subject.) Funding from the Swedish VR and SSF, and Danish Research Councils is gratefully acknowledged. D.G. acknowledges support from DFG-Centre for Functional Nanostructures and the ESF network "Arrays of Quantum Dots and Josephson Junctions".

Supporting Information Available: Textual presentation of model calculations. This material is available free of charge via the Internet at http://pubs.acs.org.

References

(1) Tao, N. J. *Nature Nanotechnol.* **2006**, *1*, 173.
(2) Ho, W. *J. Chem. Phys.* **2002**, *117*, 11033.
(3) Troisi, A.; Ratner, M. *Small* **2006**, *2*, 172.
(4) Silien, C.; Liu, N.; Ho, W.; Maddox, J. B.; Mukamel, S.; Liu, B.; Bazan, G. C. *Nano Lett.* **2008**, *8*, 208.
(5) Liljeroth, P.; Repp, J.; Meyer, G. *Science* **2007**, *317*, 1203.
(6) Choi, B.-Y.; Kahng, S.-J.; Kim, S.; Kim, H.; Kim, H. W.; Song, Y. J.; Ihm, J.; Kuk, Y. *Phys. Rev. Lett.* **2006**, *96*, 156106.
(7) Danilov, A. V.; Kubatkin, S. E.; Kafanov, S. G.; Flensberg, K.; Bjørnholm, T. *Nano Lett.* **2006**, *10*, 2184.
(8) Lörtscher, E.; Ciszek, J. W.; Tour, J.; Riel, H. *Small* **2006**, *2*, 973.
(9) Keane, Z. K.; Ciszek, J. W.; Tour, J. M.; Natelson, D. *Nano Lett.* **2006**, *6*, 1518.
(10) Huang, Z.; Xu, B.; Chen, Y.; Di Ventra, M.; Tao, N. *Nano Lett.* **2006**, *6*, 1240.
(11) Cai, L.; Cabassi, A.; Yoon, H.; Cabarcos, M.; McGuinnes, C. L.; Flatt, A. K.; Allara, D. L.; Tour, J. M.; Mayer, T. S. *Nano Lett.* **2005**, *5*, 2365.
(12) Steuerman, D. W.; Tseng, H.-R.; Peters, A. J.; Flood, A. H.; Jeppesen, J. O:.; Nielsen, K. A.; Stoddart, J. F.; Heath, J. R. *Angew. Chem. Int. Ed* **2004**, *43*, 6486.
(13) Ho, W.; Nazin, G. V.; Qiu, X. H. *Phys. Rev. Lett.* **2004**, *93*, 196806.
(14) Lewis, P. A.; Inman, C. E.; Yao, Y.; Tour, J. M.; Hutchison, J. E.; Weiss, P. S. *J. Am. Chem. Soc.* **2004**, *126*, 12214.
(15) Loppacher, Ch.; Guggisberg, M.; Pfeiffer, O.; Meyer, E.; Bammerlin, M.; Lüthi, R.; Schlittler, R.; Gimzewski, J. K.; Tang, H.; Joachim, C. *Phys. Rev. Lett.* **2003**, *90*, 066107.
(16) Heinrich, A. J.; Lutz, C. P.; Gupta, J. A.; Eigler, D. M. In *Advances in Solid State Physics*; Kramer, B., Ed.; Springer-Verlag: Berlin, 2003; Vol. 43, p 51.
(17) Heinrich, A. J.; Lutz, C. P.; Gupta, J. A.; Eigler, D. M. *Science* **2002**, *298*, 1381.
(18) Donhauser, Z. J.; Mantooth, B. A.; Kelly, K. F.; Bumm, L. A.; Monnel, J. D.; Stapleton, J. J., Jr.; Rawlett, A. M.; Allara, D. L.; Tour, J. M.; Weiss, P. S. *Science* **2001**, *292*, 2303.
(19) Ho, W.; Gaudioso, J. *Angew. Chem., Int. Ed.* **2001**, *40*, 4080.
(20) Collier, C. P.; Mattersteig, G.; Wong, E. W.; Luo, Y.; Beverly, K.; Sampaio, J.; Raymo, F. M.; Stoddart, J. F.; Heath, J. R. *Science* **2000**, *289*, 1172.
(21) Gaudioso, J.; Lauhon, L. J.; Ho, W. *Phys. Rev. Lett.* **2000**, *85*, 1918.
(22) Chen, J.; Reed, M. A.; Rawlett, A. M.; Tour, J. M. *Science* **1999**, *286*, 1550.
(23) Eigler, D. M.; Lutz, C. P.; Rudge, W. E. *Nature* **1991**, *352*, 600.
(24) Menéndez, J.; Page, J. B. In *Light Scattering in Solids VIII*; Cardona, M., Güntherodt, G., Eds.; Springer, Berlin, 2000.
(25) Degiorgi, L. *Adv. Phys.* **1998**, *47*, 207.
(26) Dresselhaus, M. S.; Dresselhaus, G.; Eklund, P. G. *Science of Fullerenes and Carbon Nanotubes*; Academic Press: New York, 1996.
(27) Wang, X. Q.; Wang, C. Z.; Ho, K. M. *Phys. Rev. B* **1993**, *48*, 1884.
(28) Adams, G. B.; Page, J. B.; Sankey, O. F.; Sinha, K.; Menendez, J.; Huffman, D. R. *Phys. Rev. B* **1991**, *44*, 4052.
(29) Joachim, C.; Gimzewski, J. K.; Schlittler, R. R.; Chavy, C. *Phys. Rev. Lett.* **1995**, *74*, 2102.
(30) Lu, X.; Grobis, M.; Khoo, K. H.; Louie, S. G.; Crommie, M. F. *Phys. Rev. B* **2004**, *70*, 115418.
(31) Lu, X.; Grobis, M.; Khoo, K. H.; Louie, S. G.; Crommie, M. F. *Phys. Rev. Lett.* **2003**, *90*, 096802.
(32) Kubatkin, S.; Danilov, A.; Hjort, M.; Cornil, J.; Brédas, J.-L.; Stuhr-Hansen, N.; Hedegård, P.; Bjørnholm, T. *Nature* **2003**, *425*, 698.
(33) Danilov, A. V.; Kubatkin, S. E.; Kafanov, S. G.; Bjørnholm, T. *Faraday Discuss.* **2005**, *131*, 337.
(34) Kubatkin, S. E.; Danilov, A. V.; Olin, H.; Claeson, T. *J. Low-Temp. Phys.* **2000**, *118*, 307.
(35) Danilov, A. V.; Golubev, D. S.; Kubatkin, S. E. *Phys. Rev. B* **2002**, *65*, 125312.
(36) The differential conductance in the low-conducting state reveals the same placement of HOMO/LUMO/LUMO+1 peaks, but the overall conductance is lower.
(37) Fulton, T. A.; Dunkleberger, L. N. *Phys. Rev. B* **1974**, *9*, 4760.
(38) Park, H.; Park, J.; Anderson, E. H.; Alivisatos, A. P.; McEuen, P. L. *Nature* **2000**, *407*, 57.
(39) Feynman, R. *Frontiers in Physics, Statistical Mechanics*; Adison-Wesley Publishing Co.: New York, 1972; p 53.
(40) Brandbyge, M.; Hedegård, P. *Phys. Rev. Lett.* **1994**, *72*, 2919.
(41) Brandbyge, M.; Hedegård, P.; Heinz, T. F.; Misewich, J. A.; Newns, D. M. *Phys. Rev. B* **1995**, *52*, 6042.
(42) Coulombeau, C.; Jobic, H.; Bernier, P.; Fabre, C.; Schütz, D.; Rassat, A. *J. Phys. Chem.* **1992**, *96*, 22.
(43) Perez-Jimenez, A. J.; Palacious, J. J.; Louis, E.; SanFabian, E.; Verges, J. A. *ChemPhysChem* **2003**, *4*, 388.
(44) Chavy, C.; Joachim, C.; Altibelli, A. *Chem. Phys. Lett.* **1993**, *214*, 569.
(45) Johnson, R. D.; Yannoni, C. S.; Dorn, Y. C.; Salem, J. R.; Bethune, D. S. *Science* **1992**, *255*, 1235.
(46) Manini, N.; Tossatti, E. *Phys. Rev. B* **1998**, *58*, 782.
(47) Tomita, S.; Andersen, J. U.; Bonderup, E.; Hvelplund, P.; Liu, B.; Brøndsted Nielsen, S.; Pedersen, U. V.; Rangama, J.; Hansen, K.; Echt, O. *Phys. Rev. Lett.* **2005**, *94*, 053002.

NL801273A